Effect of inhomogeneous magnetic flux on double-dot Aharonov–Bohm interferometer

2004 J. Phys.: Condens. Matter 16 2053

(http://iopscience.iop.org/0953-8984/16/12/014)

INSTITUTE OF PHYSICS PUBLISHING JOURNAL OF PHYSICS: CONDENSED MATTER

J. Phys.: Condens. Matter **16** (2004) 2053–2063 PII: S0953-8984(04)74288-5

Effect of inhomogeneous magnetic flux on double-dot Aharonov–Bohm interferometer

Zhi-Ming Bai[1,2], **Min-Fong Yang**[2] **and Yung-Chung Chen**[2]

[1] Physics Department, Hebei Science and Technology University, Shijiazhuang 050018, People's Republic of China
[2] Department of Physics, Tunghai University, Taichung 407, Taiwan

E-mail: baizhiming@tsinghua.org.cn, mfyang@mail.thu.edu.tw and ycchen@mail.thu.edu.tw

Received 30 December 2003
Published 12 March 2004
Online at stacks.iop.org/JPhysCM/16/2053 (DOI: 10.1088/0953-8984/16/12/014)

Abstract

The influence of the inhomogeneous distribution of the magnetic flux on quantum transport through coupled double quantum dots embedded in an Aharonov–Bohm interferometer are investigated. We show that the effective tunnelling coupling between two dots can be tuned by the magnetic flux imbalance threading two AB subrings. Thus the conductance and the local densities of states become periodic functions of the magnetic flux imbalance. Therefore, transport signals can be manipulated by adjusting the magnetic flux imbalance. Thus accurate control of the distribution of the magnetic flux is necessary for any practical application of such an Aharonov–Bohm interferometer.

1. Introduction

Due to recent advances in nanotechnologies, quantum transport through ultra-small quantum dots (QD) has drawn considerable interests in the last few decades [1]. In such small structures with geometrical dimensions smaller than the elastic mean free paths, electron transport is ballistic and its phase coherence can be sustained. To probe the coherence, interference experiments, most notably Aharonov–Bohm (AB) interferometry, are needed. The presence of conductance oscillations as a function of magnetic flux has been experimentally demonstrated for AB interferometers with one QD [2–7]. In [7], a mesoscopic Fano effect with complex Fano asymmetric parameters is observed and it is shown that the Fano effect can be a powerful tool to investigate the electron phase variation in such mesoscopic transport.

Recently, an AB interferometer containing two *coupled* QDs with a QD inserted in each arm has also been studied experimentally [8–11]. While there have already been many works on the AB interferometer containing two QDs, most of them only consider the system *without* direct coupling between dots. The particular interest in the coupled system lies in its potential

application in quantum communication [12], because entanglement of electrons is possible in the presence of direct tunnelling between dots. Just like a molecule of two atoms, two coupled QDs can form bonding and antibonding states. Therefore, such an AB interferometer can also be used to probe the phase coherence of the bonding between dots. Moreover, the possibility to control each of the two QDs separately increases the dimension of the parameter space for the transport properties compared to their single-dot AB counterparts. Thus it can be considered as the starting point of the study of an experimentally unexplored region. Motivated by these experimental works, theoretical investigations of such a system have just begun [13, 14]. It is noted in [13] that the interdot tunnelling divides the AB interferometer into two coupled subrings, and the total magnetic flux through the device is composed of magnetic flux through the two subrings. If the applied magnetic field is non-uniform and/or the construction of the AB interferometer is asymmetric, the magnetic flux threading two subrings can, in general, be different[3]. The possibility of the non-uniform distribution of magnetic flux is not taken into account in [14].

In this paper, the AB interferometer containing two *coupled* QDs is investigated and we focus our attention on the effect of inhomogeneous magnetic flux. While this effect has been studied in [13] by solving numerically the modified rate equations, they consider only a special case with integer values of the magnetic flux ratio of two subrings. Our aim is to provide general analytic expressions for the conductance and the local densities of states, which may serve as guides for both ongoing and future experimental endeavours[4].

By solving exactly a simple model system, we derive general formulae for the conductance and the local densities of states, which include most of the previous results [13, 14, 16]. Moreover, we find that non-uniform distribution of the magnetic field piercing the AB interferometer will have an important influence on electron transport. Thus complex characteristic transport features can occur, which can easily be manipulated by applied gate voltages and magnetic flux. First, the magnetic flux imbalance contributes a phase factor to the tunnelling coupling. Thus the overlapping of the dot's wavefunctions can be tuned through the phase of the interdot tunnelling matrix element by adjusting the flux imbalance. Second, the conductance and the local densities of states consist of the Breit–Wigner and Fano resonances. The corresponding Fano factors, the positions and widths of these resonances depend not only on the total magnetic flux but also on the magnetic flux imbalance. Thus electron transport can be controlled by changing both the total magnetic flux and the magnetic flux imbalance. Third, the normal AB oscillations with a period of 2π are destroyed and complex periodic oscillations can be generated. The oscillation periods for the total magnetic flux and the magnetic flux imbalance are, in general, 4π, while in some particular situations the 2π-periodicity can be recovered. Besides the 2π- and the 4π-period oscillation, if ϕ and $\delta\phi$ are not independent, the oscillating periods can have other possibilities. For the particular case where the ratio of the magnetic flux in two subrings is an integer n [13], the oscillating period becomes $2(n+1)\pi$. All of these results can be easily read off from our general analytic expressions. Furthermore, the AB oscillations can be very sensitive to the magnetic flux imbalance. Thus accurate control of the distribution of the magnetic flux is necessary for any practical application of such an AB interferometer.

[3] Here we suggest a possible way to adjust experimentally the flux imbalance in the double-dot AB interferometer. A periodic magnetic field with period about 1 μm has been generated by using a regular array of superconductors (Carmona *et al* [15]) or micromagnets (Ye *et al* [15]). By covering various periodic magnetic fields with different periods on the top of the sample with the double-dot AB interferometer, one can change to some extent the magnetic flux imbalance threading two subrings.

[4] For example, our general analytic expressions of the conductance and the local densities of states provide a better fitting formula for the experimental data as long as the flux imbalance is there. The fitting parameter of the flux imbalance can give an indication of the degree of asymmetry in the construction of the AB interferometer.

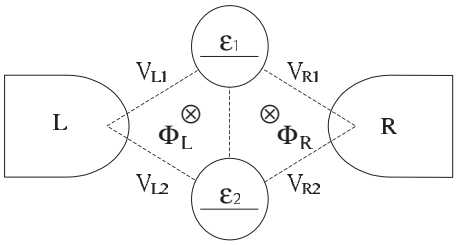

Figure 1. Schematic diagram of two transversely coupled quantum dots embedded in an Aharonov–Bohm interferometer.

The paper is organized as follows. We describe the model in section 2. The general expressions of the differential conductance and the density of states are derived there. In section 3, we evaluate the conductance as a function of the Fermi energy and show that the conductance in the present case consists of two resonances which are composed of a Breit–Wigner resonance and a Fano resonance. The local densities of states are calculated in section 4, which show similar behaviours to the conductance. In section 5, the AB oscillation of the conductance as a function of total magnetic flux and flux imbalance are studied. Finally, the results are summarized and discussed in section 6. In sections 3–5 symmetric coupling of the dots to the left and right leads is assumed for simplicity. The effect of asymmetric coupling is briefly discussed in the appendix.

2. Theory

We consider an AB geometry as depicted in figure 1, which is basically equivalent to the experimental set-up of [8]. The interdot and the intradot electron–electron interactions are neglected and only one energy level in each dot is assumed relevant. The magnetic flux threading the right-handed (left-handed) subring is denoted by Φ_{R} (Φ_{L}). Thus the total magnetic flux through the whole AB interferometer is $\Phi = \Phi_{\mathrm{L}} + \Phi_{\mathrm{R}}$. The Hamiltonian of the system can be written as

$$H = \sum_{k\alpha} \varepsilon_{k\alpha} c^{\dagger}_{k\alpha} c_{k\alpha} + \mathbf{d}^{\dagger}\mathbf{H}_0\mathbf{d} + \sum_{k\alpha} (c^{\dagger}_{k\alpha}\mathbf{V}_{k\alpha}\mathbf{d} + \mathrm{H.c.}), \tag{1}$$

where $c^{\dagger}_{k\alpha}$ ($c_{k\alpha}$) are the creation (annihilation) operators for electrons with momentum k in the leads $\alpha = \mathrm{L}, \mathrm{R}$. For convenience, we introduce the following matrix representation for the dynamics of the isolate double QDs and the tunnelling between dots and leads:

$$\mathbf{d}^{\dagger} = (d^{\dagger}_1, d^{\dagger}_2), \qquad \mathbf{d} = \begin{pmatrix} d_1 \\ d_2 \end{pmatrix},$$
$$\mathbf{H}_0 = \begin{pmatrix} \varepsilon_1 & t \\ t^* & \varepsilon_2 \end{pmatrix},$$
$$\mathbf{V}_{k\alpha} = (V_{k\alpha 1}, V_{k\alpha 2}),$$

where d_i ($d^{\dagger}_i$) annihilates (creates) an electron in the ith dot ($i = 1, 2$). The energy level in dot i is denoted by ε_i, which can be varied by the applied gate voltages. t is the interdot tunnelling coupling and $V_{k\alpha i}$ are the tunnelling matrix elements between dots and leads. The magnetic flux is described by an AB phase factor attached to the interdot tunnelling coupling and the tunnelling matrix elements. We choose a gauge such that $t = |t|\exp(\mathrm{i}\delta\phi/2)$, $V_{k\mathrm{L}1} = |V_{k\mathrm{L}1}|\exp(-\mathrm{i}\phi/4)$, $V_{k\mathrm{L}2} = |V_{k\mathrm{L}2}|\exp(\mathrm{i}\phi/4)$, $V_{k\mathrm{R}2} = |V_{k\mathrm{R}2}|\exp(-\mathrm{i}\phi/4)$ and

$V_{k\mathrm{R}1} = |V_{k\mathrm{R}1}|\exp(\mathrm{i}\phi/4)$ with the (dimensionless) total magnetic flux $\phi \equiv 2\pi\Phi/\Phi_0$ and the (dimensionless) magnetic flux imbalance $\delta\phi \equiv 2\pi(\Phi_\mathrm{L} - \Phi_\mathrm{R})/\Phi_0$, where $\Phi_0 = h/e$ is the flux quantum.

By employing the Landauer formula at zero temperature, the differential conductance G is related to the transmission $T(\omega)$ of an electron of energy ω [17]:

$$G = \frac{e^2}{h}T(\varepsilon_\mathrm{F}), \tag{2}$$

where ε_F stands for the Fermi level of both leads. The total transmission $T(\omega)$ can be expressed as

$$T(\omega) = \mathrm{Tr}\{\mathbf{\Gamma}^\mathrm{L}\mathbf{G}^\mathrm{a}(\omega)\mathbf{\Gamma}^\mathrm{R}\mathbf{G}^\mathrm{r}(\omega)\}, \tag{3}$$

where $\mathbf{G}^{\mathrm{r(a)}}(\omega)$ is the Fourier transform of the retarded (advanced) Green function of the QDs, $\mathbf{G}^{\mathrm{r(a)}}(t) = \mp\mathrm{i}\theta(\pm t)\langle\{\mathbf{d}(t), \mathbf{d}^\dagger(0)\}\rangle$, where $\theta(t)$ is the step function and the upper (lower) signs correspond to the retarded (advanced) one. The matrix $\mathbf{\Gamma}^\alpha = 2\pi\sum_k \mathbf{V}^\dagger_{k\alpha}\mathbf{V}_{k\alpha}\delta(\omega - \varepsilon_{k\alpha})$ describes the tunnelling coupling of the two QDs to the lead α. Here we neglect the energy dependence of $\mathbf{\Gamma}^\alpha$. Notice that the off-diagonal matrix elements of $\mathbf{\Gamma}^\alpha$ are complex numbers due to the AB phase factors.

By using the equation of motion method, the exact retarded (advanced) Green function of the QDs is given by

$$\mathbf{G}^{\mathrm{r(a)}}(\omega) = \frac{1}{D^{\mathrm{r(a)}}(\omega)}\begin{pmatrix} \omega - \varepsilon_2 \pm \frac{\mathrm{i}}{2}\Gamma_{22} & t \mp \frac{\mathrm{i}}{2}\Gamma_{12} \\ t^* \mp \frac{\mathrm{i}}{2}\Gamma_{21} & \omega - \varepsilon_1 \pm \frac{\mathrm{i}}{2}\Gamma_{11} \end{pmatrix}, \tag{4}$$

where

$$\begin{aligned} D^{\mathrm{r(a)}}(\omega) = {} & \left(\omega - \varepsilon_1 \pm \frac{\mathrm{i}}{2}\Gamma_{11}\right)\left(\omega - \varepsilon_2 \pm \frac{\mathrm{i}}{2}\Gamma_{22}\right) + \frac{1}{4}(|\Gamma^\mathrm{L}_{12}|^2 + |\Gamma^\mathrm{R}_{12}|^2) + \frac{1}{2}|\Gamma^\mathrm{L}_{12}||\Gamma^\mathrm{R}_{12}|\cos\phi \\ & - |t|^2 \mp \mathrm{i}|t||\Gamma^\mathrm{L}_{12}|\cos\left(\frac{\phi + \delta\phi}{2}\right) \mp \mathrm{i}|t||\Gamma^\mathrm{R}_{12}|\cos\left(\frac{\phi - \delta\phi}{2}\right) \end{aligned} \tag{5}$$

with $\mathbf{\Gamma} = \sum_\alpha \mathbf{\Gamma}^\alpha$. From the above expression, we find that the conductance depends not only on the total magnetic flux ϕ, but also on the magnetic flux imbalance $\delta\phi$ between the right and the left parts of the present double-dot AB interferometer. As mentioned before, without the interdot tunnelling coupling $|t| = 0$, there is only one loop in the AB interferometer and the transport is determined only by the phase ϕ. In the special case of zero magnetic field, our result reduces to that obtained in [16].

From equations (4) and (5), general expressions of the conductance and the local density of states can be reached. However, since we focus our attention on the effect of flux imbalance, we assume for simplicity that the magnitudes of the tunnelling matrix elements between the dots and the leads are the same. Thus all of the magnitudes $|\Gamma^\alpha_{ij}|$ become identical, which is denoted by $\Gamma/2$, while their values are not the same because of the AB phase factors. (As shown in the appendix, the following results are qualitatively unchanged even when the magnitudes of $|\Gamma^\alpha_{ij}|$ are different.) After substituting equations (3)–(5) into (2), we can obtain a compact form of the differential conductance:

$$G = \frac{e^2}{h}\frac{(e_+ - e_-)^2 + 4\Delta}{|(\mathrm{i} - e_+)(\mathrm{i} - e_-) - \Delta'|^2} \tag{6}$$

with

$$\begin{aligned} e_{\pm} &\equiv \frac{2(\bar{\varepsilon} \pm |t| \cos\frac{\delta\phi}{2} - \varepsilon_{\mathrm{F}})}{\Gamma_{\pm}}, \\ \Delta &\equiv \frac{(\delta\varepsilon)^2}{\Gamma_+\Gamma_-}, \\ \Delta' &\equiv \frac{(\delta\varepsilon)^2 + 4|t|^2 \sin^2\frac{\delta\phi}{2}}{\Gamma_+\Gamma_-}, \\ \Gamma_{\pm} &\equiv \left(1 \mp \cos\frac{\phi}{2}\right)\Gamma, \end{aligned} \tag{7}$$

where $\bar{\varepsilon} \equiv (\varepsilon_1+\varepsilon_2)/2$ and $\delta\varepsilon \equiv \varepsilon_1 - \varepsilon_2$ denote the mean energy and the energy detuning of two QDs, respectively. The parameters of e_+ and Γ_+ (e_- and Γ_-) are relevant to the antibonding (bonding) state of the QD molecule. From the above result, we find that the conductance shows oscillation patterns when either the total magnetic flux ϕ or the magnetic flux imbalance $\delta\phi$ is changed (see also section 5). We note that equation (6) becomes identical to that obtained in [14] in the special case of $\delta\phi = 0$, which will even reduce to the result obtained in [18] in the case of the absence of the interdot coupling ($t = 0$). However, when the distribution of the magnetic flux is non-uniform (i.e. $\delta\phi \neq 0$), more interesting behaviours can show up. It is clear from the expression of $e_{\pm}$ that, by adjusting the phase of the interdot tunnelling matrix element through the flux imbalance $\delta\phi$ in the AB interferometer, one can tune the overlapping of the dot's wavefunctions. Moreover, the level crossing of the bonding and the antibonding states can occur by varying $\delta\phi$. We emphasize again that these are possible only when interdot tunnelling coupling is nonzero.

The local density of states at the ith QD is given by $\rho_i(\omega) = -\mathrm{Im}G^{\mathrm{r}}_{ii}(\omega)/\pi$. By using the expression of the retarded Green function in equation (4), the general formula of the local densities of states at ε_{F} can be written as

$$\rho_{1(2)}(\varepsilon_{\mathrm{F}}) = \frac{\Gamma_+ e_+^2 + \Gamma_- e_-^2 + (\Gamma_+ + \Gamma_-)(1+\Delta') \mp 2\delta\varepsilon(e_+ + e_-)}{2\pi\Gamma_+\Gamma_-|(\mathrm{i} - e_+)(\mathrm{i} - e_-) - \Delta'|^2}, \tag{8}$$

where the upper (lower) sign corresponds to ρ_1 (ρ_2). Because most of the parameters defined in equation (7) depend on ϕ and/or $\delta\phi$, the local densities of states ρ_1 and ρ_2 again have oscillating behaviours as the total magnetic flux and/or the magnetic flux imbalance are varied.

3. Conductance

The general form of the conductance in equation (6) is quite similar to that obtained in [14] for the $\delta\phi = 0$ case. Therefore, following the same kind of analysis, one can easily show that the conductance in the present case consists of two resonances which are composed of a Breit–Wigner resonance and a Fano resonance.

Without loss of generality, we can discuss the case in the limit $\Gamma_- \gg \Gamma_+$. If the energy scale is larger than Γ_+ ($|e_+| \gg 1$), the conductance in equation (6) indeed takes the Breit–Wigner form:

$$G \simeq G_{\mathrm{BW}} = \frac{e^2}{h}\frac{1}{e_-^2 + 1}. \tag{9}$$

Its width is Γ_- which depends on the total magnetic flux but not on the flux imbalance (see equation (7)). Near the narrower resonance regime ($|e_+| \lesssim 1$), the conductance does show the Fano resonance behaviour:

$$G \simeq G_{\mathrm{Fano}} = \frac{e^2}{h} T_{\mathrm{b}} \frac{|e'_+ + Q|^2}{{e'_+}^2 + 1}, \tag{10}$$

where the background transmission is given by $T_b = 1/(q^2+1)$ with $q = 4|t|\cos(\delta\phi/2)/\Gamma_-$ and

$$e'_+ = \frac{e_+ + qT_b\Delta'}{1+T_b\Delta'}. \tag{11}$$

The modified Fano factor is now given by

$$Q = q\frac{1-T_b\Delta'}{1+T_b\Delta'} + i\frac{2\sqrt{\Delta}}{1+T_b\Delta'}, \tag{12}$$

and the width of the Fano resonance becomes $\Gamma'_+ = \Gamma_+(1+T_b\Delta')$. While these results are formally identical to those obtained in [14], we show that the modified Fano factor, the position and width of the resonance all depend not only on the total magnetic flux ϕ, but also on the magnetic flux imbalance $\delta\phi$. Thus transport signals can be manipulated by adjusting both ϕ and $\delta\phi$.

For the perfectly symmetrical geometry (i.e. $\delta\varepsilon = 0$ and $|\Gamma^{\alpha}_{ij}|$ are all the same) and in the case of zero magnetic field (or more generally $|\cos(\phi/2)| = 1$ and $|\cos(\delta\phi/2)| = 1$), the width of the Fano resonance becomes zero (or the lifetime of the antibonding state becomes infinitely long). It is because the antibonding state now becomes totally decoupled to the leads. Therefore, the Fano resonance will disappear in this case. This phenomena had been pointed out a decade ago [19], which is recently called as a 'ghost of Fano resonance' [16]. We note that this disappearance of the Fano resonance can happen only in this very special case. For example, even for the perfectly symmetrical geometry, the Fano resonance will show up when the magnetic field is turned on (see also the appendix).

To illustrate the above discussions, the differential conductance G as a function of the Fermi energy ε_F is shown in figure 2 for various $\delta\phi$ with $|t|/\Gamma = 1$, $\delta\varepsilon = 0$ (the so-called 'covalent limit') and $\phi = 0.3\pi$. Here $\bar{\varepsilon}$ is taken as the zero-energy level. Figure 2(a) reproduces the topmost one of figure 2 in [14]. We find that, as $\delta\phi$ increases from zero to π, two resonances come closer and closer, and finally two energy levels of resonance meet each other when $\delta\phi = \pi$. This can be understood from the expressions of e_- and e'_+. For a further increase of $\delta\phi$, the Breit–Wigner resonance keeps moving to the positive-energy side while the Fano resonance goes to the negative-energy side. The resonance levels will move back when $\delta\phi > 2\pi$ and the curve for $\delta\phi = 0$ is recovered when $\delta\phi$ is increased to 4π. Thus the conductance has in general a period of 4π for $\delta\phi$ (for further discussions, see section 5).

In figure 2, we find that the zero and the full transmission can occur at some particular values of the Fermi energies. The analytic expressions of these Fermi energies can be easily derived. From equations (6) and (7), it is obvious that, if the two levels of the double QDs are not the same ($\delta\varepsilon \neq 0$), the conductance cannot be zero. In this case, $\Delta \neq 0$ and the modified Fano factor in equation (12) becomes a complex number. It means that the completely destructive interference in the present AB interferometer will not appear in this case. However, when $\delta\varepsilon = 0$, the completely destructive interference and transmission zero happen at the Fermi energy

$$\varepsilon_F = \bar{\varepsilon} + |t|\cos\frac{\delta\phi}{2}\Big/\cos\frac{\phi}{2}, \tag{13}$$

provided that $\sin(\phi/2) \neq 0$ or $\sin(\delta\phi/2) \neq 0$. It is sensitive to the total magnetic flux ϕ and the magnetic flux imbalance $\delta\phi$. On the other hand, the conductance can reach its quantum limit $G = e^2/h$ at the Fermi energies

$$\varepsilon_F = \bar{\varepsilon} \pm \sqrt{\left(\frac{\delta\varepsilon}{2}\right)^2 + |t|^2 - \left(\frac{\Gamma}{2}\right)^2 \sin^2\frac{\phi}{2}} \tag{14}$$

if $\sin(\phi/2)\sin(\delta\phi/2) = 0$ and the expression in the square root is positive. The last term in the square root of equation (14) gives the so-called 'flux-dependent level attraction' mentioned

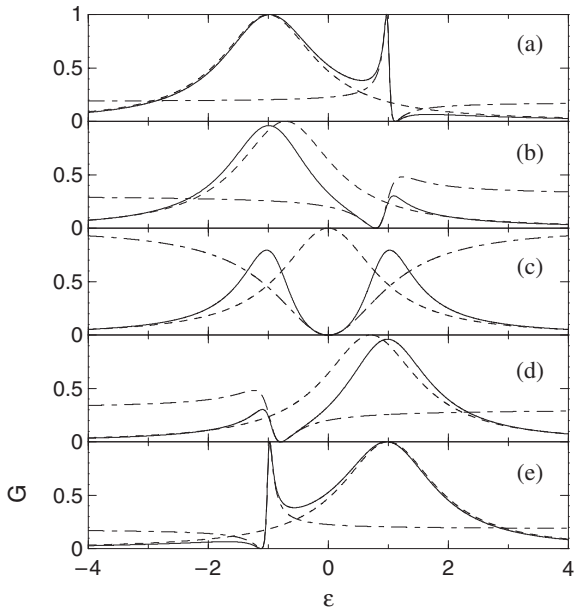

Figure 2. Differential conductance G in units of e^2/h (full curves) as a function of the Fermi energy (in units of Γ) for various flux imbalances. The results shown in panels (a)–(e) correspond to the flux imbalances $\delta\phi = 0, \pi/2, \pi, 3\pi/2$ and 2π. Other parameters are given by $\bar{\varepsilon} = \delta\varepsilon = 0$, $|t|/\Gamma = 1$ and $\phi = 0.3\pi$. Broken and chain curves denote the Breit–Wigner and the generalized Fano asymptote given in equations (9) and (10), respectively.

in [18]. From the above discussion it is realized that the value of transmission will in general not be zero or one unless some particular conditions happen to be satisfied[5].

4. Local density of states

Similar behaviours to the results in the previous section can be found by examining the local density of states in each of the quantum dots.

For the perfectly symmetrical geometry, $\delta\varepsilon = 0$ and $\delta\phi = 0$. Therefore $\Delta = \Delta' = 0$ and equation (8) reduces to

$$\rho_1 = \rho_2 = \frac{1}{2\pi\Gamma_-(e_-^2+1)} + \frac{1}{2\pi\Gamma_+(e_+^2+1)}. \tag{15}$$

That is, both of the local densities of states take the form of the superposition of two Breit–Wigner resonances of widths Γ_- and Γ_+ at the bonding and antibonding energies, respectively. However, in other cases, following the same kind of analysis in the previous section, it can be shown that the local densities of states consist of a Breit–Wigner at the bonding energy and a Fano lineshape at the antibonding energy.

Without loss of generality, we discuss the case again in the limit $\Gamma_- \gg \Gamma_+$. If the energy scale is larger than Γ_+ ($|e_+| \gg 1$), both of the local densities of states in equation (8) take the

[5] Similar expressions of the Fermi energies corresponding to the zero and the full transmission have been given in [16] and [18] for various limiting cases. By taking $\delta\phi = 0$ and $t = 0$, equation (14) reduces to the condition of full transmission given in [18]. On the other hand, when the magnetic field is absent and the set-up is perfectly symmetrical, i.e. $\phi = \delta\phi = 0$ and $\delta\varepsilon = 0$, equations (13) and (14) can be related to those in [16].

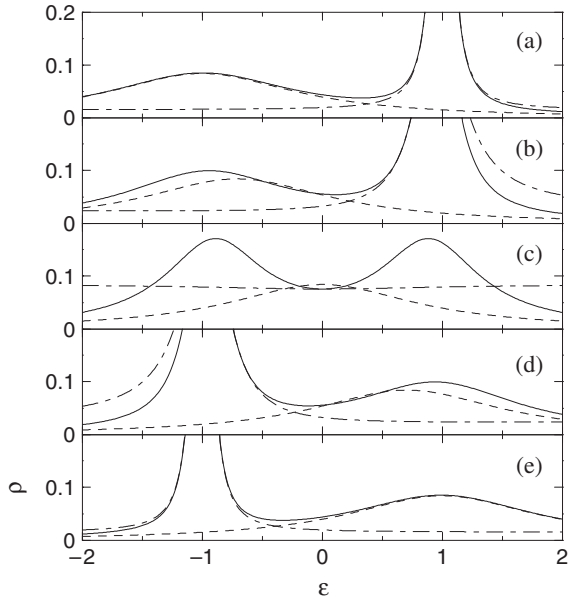

Figure 3. Local density of states at a QD as a function of the Fermi energy (in units of Γ). The results shown in panels (a)–(e) correspond to the flux imbalances $\delta\phi = 0, \pi/2, \pi, 3\pi/2$ and 2π. Other parameters are the same as those used in figure 2. Broken and chain curves denote the Breit–Wigner and the generalized Fano asymptote given in equations (16) and (17), respectively.

Breit–Wigner form of width Γ_-:

$$\rho_{1(2)} \simeq \frac{1}{2\pi\Gamma_-(e_-^2+1)}. \tag{16}$$

Near the narrower resonance regime ($|e_+| \lesssim 1$), the local densities of states show the Fano resonance behaviour:

$$\rho_{1(2)} \simeq \rho_{\rm b}\frac{|e'_+ - P_{1(2)}|^2}{1+e'^2_+}, \tag{17}$$

where $\rho_{\rm b} \equiv T_{\rm b}/(2\pi\Gamma_-)$ and the corresponding Fano factor is

$$P_{1(2)} = \frac{qT_{\rm b}\Delta' \pm \sqrt{\Delta\frac{\Gamma_-}{\Gamma_+}}}{1+T_{\rm b}\Delta'} + {\rm i}\frac{\sqrt{\left[\left(q \pm \sqrt{\Delta\frac{\Gamma_+}{\Gamma_-}}\right)^2 + (1+\Delta'-\Delta)\left(1+\frac{\Gamma_+}{\Gamma_-}\right)\right]\frac{\Gamma_-}{\Gamma_+}}}{1+T_{\rm b}\Delta'}, \tag{18}$$

where the upper (lower) sign corresponds to P_1 (P_2). The Fano factor in equation (18) is more complicated than that for the conductance (equation (12)). Thus it is possible in some situations (say, $\Delta = 0$) that $P_{1(2)}$ is a complex number but Q is real. Notice that the present Fano factors are in general not the same for different QDs. From the above results, it can be understood that the Fano factor $P_{1(2)}$, the position and width of the resonance can all be manipulated by adjusting both the total magnetic flux ϕ and the magnetic flux imbalance $\delta\phi$. In the absence of the magnetic field, the above expressions are equivalent to equations (27) and (28) of [16].

The local density of states of as a function of Fermi energy $\varepsilon_{\rm F}$ is plotted in figure 3 for the same parameters used in figure 2. In this case, $\rho_1 = \rho_2$. We find that the same level crossing appears as $\delta\phi$ is varied and the curve again has a period of 4π for $\delta\phi$ (for further discussions,

see section 5). We notice that the local density of states is always nonvanishing for the chosen parameters, because the Fano factor $P_{1(2)}$ is complex in these cases. As compared with figure 2, it is found that the states with small density of states can have almost full transmission and those with large density of states can show zero transmission. This indicates that the full and the zero transmission are indeed consequences of the quantum interference, as mentioned before.

5. Aharonov–Bohm oscillations

We now discuss the AB oscillation of the conductance as a function of total magnetic flux ϕ and the magnetic flux imbalance $\delta\phi$ with fixed mean energy $\bar{\varepsilon}$ and energy detuning $\delta\varepsilon$ of two QDs.

From equation (6), it is clear that the conductance (and also the local densities of states, see equation (8)) is a periodic function of both ϕ and $\delta\phi$. The oscillation periods for ϕ and $\delta\phi$ are in general 4π. The 4π-period oscillation for $\delta\phi$ has been implied in figure 2, and the 4π-period oscillation for ϕ in the case of $\delta\phi = 0$ has been found in [14]. However, in the following particular situations, the 2π-periodicity can occur.

(i) If we take $\varepsilon_F = \bar{\varepsilon}$, then $\Gamma_+ e_+ = -\Gamma_- e_- = 2|t|\cos(\delta\phi/2)$. In this case, one can show that the conductance is now a function of $\cos^2(\phi/2)$ and $\cos^2(\delta\phi/2)$. Hence the conductance shows 2π-period oscillation[6]. This 2π-period oscillation for $\delta\phi$ can be understood from figure 2, if we trace the change of G at $\varepsilon_F = \bar{\varepsilon} = 0$ as $\delta\phi$ is varied from 0 to 2π.

(ii) If $\delta\phi = \pi$ (or more generally $\cos(\delta\phi/2) = 0$), we have $\Gamma_+ e_+ = \Gamma_- e_- = 2(\bar{\varepsilon} - \varepsilon_F)$. Therefore, the conductance becomes a function of $\cos^2(\phi/2)$ and the oscillation periods for ϕ is 2π.

(iii) If $\phi = \pi$ (or more generally $\cos(\phi/2) = 0$), we have $\Gamma_+ = \Gamma_- = \Gamma$. In this case, the conductance is a function of $\cos^2(\delta\phi/2)$ with a 2π-period oscillation for $\delta\phi$.

As an illustration, the AB oscillation as a function of ϕ is shown in figure 4 for different values of $\delta\phi$ with $|t|/\Gamma = 0.3$ and $\delta\varepsilon/\Gamma = 0.1$. Here we choose $\varepsilon_F = \bar{\varepsilon} - \sqrt{(\delta\varepsilon/2)^2 + |t|^2}$, which is the energy for the bonding state when the QDs are decoupled to the leads. $\bar{\varepsilon}$ is again taken as the zero-energy level for convenience. The curve for $\delta\phi = 0$ corresponds to the $A1$ curve in figure 4(c) of [14], where sharp peaks around $\phi = 4n\pi$ ($n = 0, \pm1, \pm2, \ldots$) result. It shows that the conductance can be very sensitive to the total magnetic flux ϕ for the chosen parameters (say, near $\phi = 0$). This opens the possibility to manipulate transport in a nontrivial way by varying the magnetic field. As shown in figure 4, we see that this sensitivity can even be strengthened when $\delta\phi$ is present. As $\delta\phi$ increases to π, the periodicity even changes from 4π to 2π, as discussed above.

Besides the 2π- and 4π-period oscillation studied above, it is found that, if ϕ and $\delta\phi$ are not independent, the oscillating periods can have other possibilities [13]. The authors of [13] show numerically that the oscillating period will be $2(n+1)\pi$ when $\delta\phi = [(n-1)/(n+1)]\phi$ (or the magnetic flux ratio $\Phi_L/\Phi_R = n$) with n being integers. This result can be easily explained from our analytic expression of equation (6). As ϕ is being varied from 0 to $2(n+1)\pi$, $\delta\phi$ is increased from 0 to $2(n-1)\pi$ and therefore we have $\Gamma_\pm \to \Gamma_\pm$, $e_\pm \to e_\pm$ ($\Gamma_\pm \to \Gamma_\mp$, $e_\pm \to e_\mp$) and $\Delta' \to \Delta'$ if n is odd (even). This puts G back to its original value. It means that the oscillating period is $2(n+1)\pi$ in this case.

[6] In this case, the total density of states, $\rho_1 + \rho_2$, has also 2π-oscillating periods for ϕ and $\delta\phi$. However, the oscillating periods for ϕ and $\delta\phi$ of the *local* densities of states, ρ_1 and ρ_2, are still 4π unless $\Delta = 0$ (i.e. the energy detuning $\delta\varepsilon = 0$).

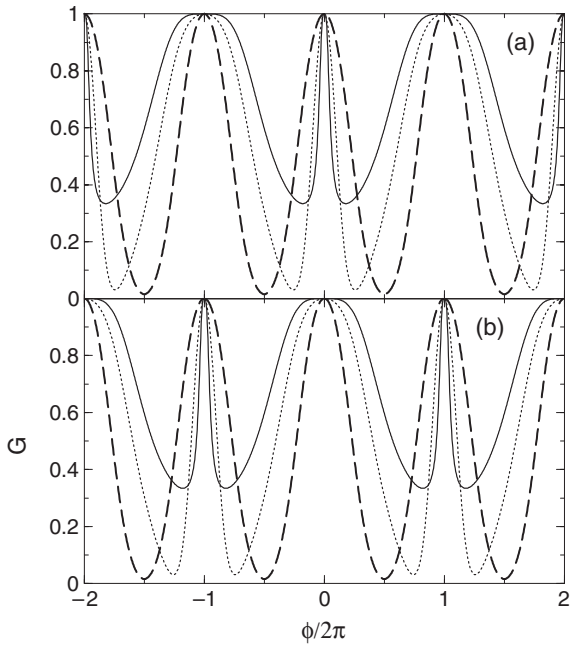

Figure 4. AB oscillations as a function of the total magnetic flux ϕ for various flux imbalances $\delta\phi$. (a) $\delta\phi = 0$ (full curve), $\pi/2$ (dotted curve), π (broken curve). (b) $\delta\phi = \pi$ (broken curve), $3\pi/2$ (dotted curve) and 2π (full curve). Here the Fermi energy is taken as the energy for the bonding state when the QDs are decoupled to the leads (see the text). Other parameters are given by $\bar{\varepsilon} = 0$, $|t|/\Gamma = 0.3$, $\delta\varepsilon/\Gamma = 0.1$.

6. Conclusions

In conclusion, we have investigated the influence of the non-uniform distribution of the magnetic flux on quantum transport through coupled double QDs embedded in an AB interferometer. We show that the effective tunnelling coupling between two dots can be tuned by the magnetic flux imbalance $\delta\phi$ threading two AB subrings. Therefore, the conductance and the local densities of states become periodic functions of $\delta\phi$. Moreover, the conductance and the local densities of states are shown to be composed of a Breit–Wigner resonance and a Fano resonance. The corresponding Fano factors, the positions and widths of the resonances all depend not only on ϕ but also on $\delta\phi$. Thus transport signals can be manipulated by adjusting both ϕ and $\delta\phi$. Finally, we point out that the AB oscillations can be very sensitive to $\delta\phi$. Thus accurate control of the distribution of the magnetic flux is necessary for any practical application of such an AB interferometer.

Acknowledgments

ZMB's work is financially supported partly by grant no. NSC-91-2816-M-029-0002-6. MFY is supported by grant no. NSC 91-2112-M-029-007. YCC acknowledges financial support by grant no. NSC 91-2112-M-029-006.

Appendix. Effect of asymmetric coupling between dots and leads

In this appendix, we devote ourselves to the effect of differences in the matrix elements of Γ^{α}_{ij}. As an example, we follow the set-up which is considered in [16] in the case of zero magnetic

field: $\Gamma_{11}^{\mathrm{R}} = \Gamma_{22}^{\mathrm{L}} \equiv \gamma_1$ and $\Gamma_{11}^{\mathrm{L}} = \Gamma_{22}^{\mathrm{R}} \equiv \gamma_2$, and the magnitudes of the off-diagonal matrix elements $|\Gamma_{21}^{\mathrm{L}}| = |\Gamma_{12}^{\mathrm{L}}| = |\Gamma_{21}^{\mathrm{R}}| = |\Gamma_{12}^{\mathrm{R}}| \equiv \sqrt{\gamma_1\gamma_2}$.

In this case, the conductance and the local densities of states are again given by equations (6) and (8), respectively, where $e_\pm$ and Δ' are identical to those given in equation (7), but Δ and $\Gamma_\pm$ now become:

$$\Delta = \left[\frac{2(\gamma_1-\gamma_2)|t|\sin\frac{\delta\phi}{2} - 2\sqrt{\gamma_1\gamma_2}\delta\varepsilon\sin\frac{\phi}{2}}{\Gamma_+\Gamma_-}\right]^2, \tag{A.1}$$

$$\Gamma_\pm = (\gamma_1+\gamma_2) \mp 2\sqrt{\gamma_1\gamma_2}\cos\frac{\phi}{2}. \tag{A.2}$$

When $\gamma_1 = \gamma_2 \equiv \Gamma/2$, the above expressions reduce to the corresponding ones in equation (7). Thus, merely by replacing the functional forms of Δ and $\Gamma_\pm$, the discussions in the text are still applied in this case of asymmetric coupling between dots and leads. From equation (A.2), one finds that, when $\phi = 0$, Γ_+ approaches zero as $\gamma_1 - \gamma_2 \to 0$. This result had been pointed out in [19]. However, for nonzero magnetic field, none of $\Gamma_\pm$ will be zero in the limit $\gamma_1 - \gamma_2 \to 0$ as long as $|\cos\frac{\phi}{2}| \neq 1$. Thus the phenomena of a 'ghost of Fano resonance' [16] will not appear when the magnetic field is nonzero.

References

[1] Sohn L L, Kouwenhoven L P and Schön G (ed) 1997 *Mesoscopic Electron Transport* (Dordrecht: Kluwer)
Grabert H and Devoret M H (ed) 1991 *Single Charge Tunnelling* (New York: Plenum)
Averin D V and Likharev K K 1991 *Mesoscopic Phenomena in Solids* ed B L Altshuler, P A Lee and R A Webb (Amsterdam: Elsevier) pp 173–271

[2] Yacoby A, Heiblum M, Mahalu D and Shtrikman H 1995 *Phys. Rev. Lett.* **74** 4047

[3] Schuster R, Buks E, Heiblum M, Mahalu D, Umansky V and Shtrikman H 1997 *Nature* **385** 417

[4] Ji Y, Heiblum M, Sprinzak D, Mahalu D and Shtrikman H 2000 *Science* **290** 779
Ji Y, Heiblum M and Shtrikman H 2002 *Phys. Rev. Lett.* **88** 076601

[5] van der Wiel W G, De Franceschi S, Fujisawa T, Elzerman J M, Tarucha S and Kouwenhoven L P 2000 *Science* **289** 2105

[6] Kobayashi K, Aikawa H, Katsumoto S and Iye Y 2002 *J. Phys. Soc. Japan* **71** L2094–7
Aikawa H, Kobayashi K, Sano A, Katsumoto S and Iye Y 2003 *Preprint* cond-mat/0309084

[7] Kobayashi K, Aikawa H, Katsumoto S and Iye Y 2002 *Phys. Rev. Lett.* **88** 256806 (*Preprint* cond-mat/0309570)

[8] Holleitner A W, Decker C R, Qin H, Eberl K and Blick R H 2001 *Phys. Rev. Lett.* **87** 256802

[9] Holleitner A W, Blick R H, Hüttel A K, Eberl K and Kotthaus J P 2002 *Science* **297** 70

[10] Blick R H, Hüttel A K, Holleitner A W, Höhberger E M, Qin H, Kirschbaum J, Weber J, Wegscheider W, Bichler M, Eberl K and Hotthaus J P 2003 *Physica* E **16** 76

[11] Sigrist M, Fuhrer A, Ihn T, Ensslin K, Wegscheider W and Bichler M 2003 *Preprint* cond-mat/0307269
Sigrist M, Fuhrer A, Ihn T, Ensslin K, Ulloa S E, Wegscheider W and Bichler M 2003 *Preprint* cond-mat/0308223

[12] Loss D and Sukhorukov E V 2000 *Phys. Rev. Lett.* **84** 1035

[13] Jiang Z T, You J Q, Bian S B and Zheng H Z 2002 *Phys. Rev.* B **66** 205306

[14] Kang K and Cho S Y 2002 *Preprint* cond-mat/0210009

[15] Carmona H A *et al* 1995 *Phys. Rev. Lett.* **74** 3009
Ye P D *et al* 1995 *Phys. Rev. Lett.* **74** 3013

[16] Ladrón de Guevara M L, Claro F and Orellana P A 2003 *Phys. Rev.* B **67** 195335 There are some typographic errors in their equations (9), (10), (14) and (15)

[17] Meir Y and Wingreen N 1992 *Phys. Rev. Lett.* **68** 2512
Jauho A P, Wingreen N S and Meir Y 1994 *Phys. Rev.* B **50** 5528

[18] Kubala B and König J 2002 *Phys. Rev.* B **65** 245301

[19] Shahbazyan T V and Raikh M E 1994 *Phys. Rev.* B **49** 17123